Fuzzy Gain Scheduling Based Optimally Tuned PID Controllers for an Unmanned Underwater Vehicle

Darshana Makavita, Hung Duc Nguyen and Dev Ranmuthugala
Australian Maritime College (AMC),
An Institute of the University of Tasmania (UTAS),
Launceston, Australia.
charitam@amc.edu.au

Abstract— **Controlling the motion of an unmanned underwater vehicle is a challenging task due to the coupled, nonlinear six degrees-of-freedom vehicle dynamics. This motion is exacerbated in underactuated vehicles, as the number of actuators is less than the number of degrees-of-freedom. In this paper a three thruster Remotely Operated Vehicle is considered with the two horizontal thrusters causing disturbance on the pitch, thus creating a large coupling effect that tends to destabilize the vehicle in the vertical plane. Optimization algorithms were used with a nonlinear model to tune PID controllers for depth and heading control in the presence of measurement noise. The results for the depth control show that while the behavior is satisfactory at and around the operating point, it deteriorates further away from that point. An adequate response throughout the operational range is achieved by designing multiple optimized controllers at several operating points and gain scheduling for intermediate points. Finally a fuzzy supervisor was designed to carry out the inferencing based on the operating conditions and a set of rules.**

Keywords- unmanned underwater vehicle, ROV, PID, multiple controllers, fuzzy, optimization

I. INTRODUCTION

Unmanned Underwater Vehicles (UUVs) are increasingly used within the maritime industry for a range of missions that are hazardous or difficult for humans to carry out. These include military, scientific, and industrial applications such as: environmental monitoring, underwater inspection of estuaries and harbors, pipeline and subsea inspections, geological and biological surveys, marine habitat mapping, surveillance, etc.

The control of underwater vehicles is a complex and nonlinear problem, with many techniques employed over the years to provide stable and efficient solutions. One approach is to linearize the equations of motion of the vehicle around several operating points, which are usually differentiated by the different surge velocities associated with the motion. The most basic control structure is to use Proportional-Derivative (PD) or Proportional-Integral-Derivative (PID) controllers [1, 2]. The simple structure and relative effectiveness under normal operating conditions make them the most favoured for industrial underwater vehicles. The disadvantage of this type of controller is that they are unable to account for the nonlinearities of the system, thus they can result in inadequate performance and even instability when undergoing extreme maneuvers. A linear controller sequence of Proportional (P) and Proportional-Integral (PI) controller is suggested in [3] to control the position and velocity of the vehicle in the surge direction. The design is validated using experimental work on a THETIS UUV. A PID control method based on linearized control was proposed by Koh, et al. [4], where successful heading and depth control was demonstrated by numerical simulations and physical tests in controlled environments.

Sliding Mode Control (SMC) is another successful method tested on UUVs and is recognized for its robust performance in face of unknown vehicle dynamics and environmental disturbances. Yoerger, et al. [5] designed a SMC for their NPS ARIES UUV by initially linearizing the equations around a fixed surge velocity. This work inspired many other developments in controllers for underwater vehicles, such as those described in [6] and [7] demonstrating experimental results for full control of a UUV using SMC. The main disadvantage of SMC is that they can fall prey to chatter, which is a high frequency signal generated as a consequence of switching action.

Other control methodologies have been developed and implemented successfully in UUV control. Gain scheduling $H\infty$ controllers is one such method described in [8], with robust performance in face of plant uncertainty being a major advantage. Pascoal, et al. [9] conducted successful experiments using output feedback control on their INFANTE UUV with good results. They used linear matrix inequality (LMI)-based techniques to design a group of linear output feedback controllers, which were then scheduled based on the surge velocity of the vehicle. In [10] they gave an overview of the work that was done on the INFANTE UUV as well as highlighting the problems encountered with control and navigation of the UUV.

Another approach that is gaining popularity is the use of intelligent control methods. Foremost among them is fuzzy logic control systems, which are establishing themselves in many control fields due to their ability to capture the heuristic nature of control strategy. Chang, et al. [11] used the Takagi-Sugeno (T-S) type fuzzy model to describe their nonlinear UUV control system, while Jun, et al. [12] proposed a T–S fuzzy–model-based controller for the depth control of an

Autonomous Underwater Vehicle (AUV) in the presence of parametric uncertainties.

This work at UTAS/AMC focuses on the development of a three thruster Remotely Operated Vehicle (ROV) with haptic and adaptive control as well as an accompanying virtual reality simulator (Fig 1). This paper describes the design of a heading and depth controller for the ROV. While linearization has been the norm in the design of PID controllers, they do not perform adequately in the presence of nonlinearities. It is proposed to use the full nonlinear model in the design of the controller by using optimization tools that will treat the gains of the controller as design variables. The resulting optimized controller is compared with classical tuning rules to show its superior performance. For the depth control, fuzzy gain scheduling of optimally tuned PID controllers has been applied. The design is subjected to random noise to demonstrate its robustness to measurement noise. The controllers have been tested using a nonlinear numerical model of the ROV in a MATLAB/Simulink simulation, with the gains tuned using various optimization toolboxes available within MATLAB while the fuzzy inference mechanism is designed using the fuzzy logic toolbox.

II. KINEMATIC AND DYNAMIC MODEL

A. Reference Frame

It is convenient to use two reference frames to model the dynamics of a UUV, i.e. an Earth-fixed reference frame $\{E\}$ and a body-fixed reference frame $\{B\}$ as shown in Fig 1. The $\{E\}$-frame is coupled to the Earth, where the *x*-axis (X_e) points to the north, the *y*-axis (Y_e) to the east, and the *z*-axis (Z_e) to the center of the Earth. The $\{B\}$-frame is coupled to the vehicle, where the *x*-axis (X_b) points to the forward direction, the *y*-axis (Y_b) to the right of the vehicle, and the *z*-axis (Z_b) vertically down. The latter frame acts as the moving frame.

B. UUV Kinematics

The general motion of a UUV in six degrees-of-freedom (6DOF) is modelled by using the notation presented by Fossen [13]. The six coordinates in the $\{E\}$ frame are represented by the vector $\eta = [n \quad e \quad d \quad \phi \quad \theta \quad \psi]^T$ where $\eta_1 = [n \quad e \quad d]^T$ denote the North–East–Down (NED) positions and $\eta_2 = [\phi \quad \theta \quad \psi]^T$ are the Euler angles. The six coordinates in the $\{B\}$ frame are represented by the vector $v = [u \quad v \quad w \quad p \quad q \quad r]^T$ where $v_1 = [u \quad v \quad w]^T$ are the linear velocities and $v_2 = [p \quad q \quad r]^T$ angular velocities. The 6-DOF kinematics equations for the UUV is given by,

$$\dot{\eta} = J(\eta)v \tag{1}$$

where

$$J(\eta) = \begin{bmatrix} R_B^n(\Theta) & 0_{3\times3} \\ 0_{3\times3} & T_\Theta(\Theta) \end{bmatrix} \tag{2}$$

and

$$R_B^n(\Theta) = \begin{bmatrix} c\psi c\theta & -s\psi c\phi + c\psi s\phi s\theta & s\psi s\phi + c\psi c\phi s\theta \\ s\psi c\theta & c\psi c\phi + s\psi s\phi s\theta & -c\psi s\phi + s\psi c\phi s\theta \\ -s\theta & s\phi c\theta & c\phi c\theta \end{bmatrix} \tag{3}$$

$$T_\Theta(\Theta) = \begin{bmatrix} 1 & s\phi t\theta & c\phi t\theta \\ 0 & c\phi & -s\phi \\ 0 & s\phi/c\theta & c\phi/c\theta \end{bmatrix} \quad \theta \neq \pm 90^0 \tag{4}$$

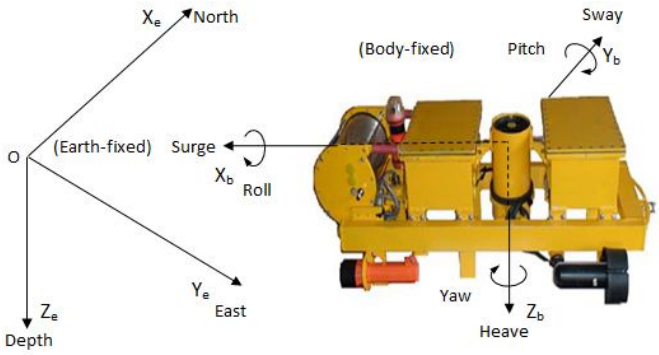

Fig. 1: AMC three tthruster ROV showing the Earth fixed and Body fixed reference frames.

C. UUV Dynamics

According to Fossen [13], the Newton's second law can be expressed in an arbitrary body-fixed coordinate frame as,

$$M_{RB}\dot{v} + C_{RB}(v)v + M_A\dot{v} + C_A(v)v + D(v)v + g(\eta) = \tau \tag{5}$$

where M_{RB} is the mass inertia matrix. $C_{RB}(v)$ is the Coriolis and Centripetal matrix.M_A and $C_A(v)$ represent the added mass and hydrodynamic Coriolis matrices respectively which are generated by the forced motion of the vehicle body. For a UUV it is customary to consider a diagonal M_A, thus,

$$M_A = -\begin{bmatrix} X_{\dot{u}} & 0 & 0 & 0 & 0 & 0 \\ 0 & Y_{\dot{v}} & 0 & 0 & 0 & 0 \\ 0 & 0 & Z_{\dot{w}} & 0 & 0 & 0 \\ 0 & 0 & 0 & K_{\dot{p}} & 0 & 0 \\ 0 & 0 & 0 & 0 & M_{\dot{q}} & 0 \\ 0 & 0 & 0 & 0 & 0 & N_{\dot{r}} \end{bmatrix} \tag{6}$$

while

$$C_A(v) = \begin{bmatrix} 0 & 0 & 0 & 0 & -Z_{\dot{w}}w & Y_{\dot{v}}v \\ 0 & 0 & 0 & Z_{\dot{w}}w & 0 & -X_{\dot{u}}u \\ 0 & 0 & 0 & -Y_{\dot{v}}v & X_{\dot{u}}u & 0 \\ 0 & -Z_{\dot{w}}w & Y_{\dot{v}}v & 0 & -N_{\dot{r}}r & M_{\dot{q}}q \\ Z_{\dot{w}}w & 0 & -X_{\dot{u}}u & N_{\dot{r}}r & 0 & -K_{\dot{p}}p \\ -Y_{\dot{v}}v & X_{\dot{u}}u & 0 & -M_{\dot{q}}q & K_{\dot{p}}p & 0 \end{bmatrix} \tag{7}$$

where $X_{\dot{u}}$ and $Y_{\dot{v}}$ and so forth are the zero-frequency added mass coefficients.The gravitational force will act through the center of gravity (CG) while the buoyancy force will act through the center of buoyancy (CB). For this ROV, the submerged weight of the body *W* is equal to the buoyancy

force *B*. Assuming that CG coincides with the origin of the body-fixed reference frame (i.e. x_g=0, y_g=0, and z_g=0), CG and CB are offset only in the z directions denoted by z_b . Thus, it can be shown that the restoring forces and moments matrix $g(\eta)$ is,

$$g(\eta) = \begin{bmatrix} 0 \\ 0 \\ 0 \\ -(z_b B)\cos(\theta)\sin(\phi) \\ (-z_b B)\sin(\theta) \\ 0 \end{bmatrix} \quad (8)$$

The damping forces on the UUVs can be written as the sum of the linear damping terms and the nonlinear quadratic damping terms. Again for underwater vehicles it is customary to consider only a diagonal damping matrix [13], i.e.

$$D(v) = \begin{bmatrix} X_u + X_{u|u|}|u| & 0 & 0 & 0 & 0 & 0 \\ 0 & Y_v + Y_{v|v|}|v| & 0 & 0 & 0 & 0 \\ 0 & 0 & Z_w + Z_{w|w|}|w| & 0 & 0 & 0 \\ 0 & 0 & 0 & K_p + K_{p|p|}|p| & 0 & 0 \\ 0 & 0 & 0 & 0 & M_q + M_{q|q|}|q| & 0 \\ 0 & 0 & 0 & 0 & 0 & N_r + N_{r|r|}|r| \end{bmatrix} \quad (9)$$

where X_u and Yv and so forth are constant linear damping coefficients and $X_{u|u|}$ and $Y_{v|v|}$ and so forth are constant quadratic damping coefficients .

III. YAW AND DEPTH CONTROLLER DESIGN

A. *Design Procedure*

The heading and depth controller was designed as follows:

a) Design an optimal PID controller at a selected operating point of the vehicle.
b) Test the controller to see feasibility of using a single optimal PID controller throughout the operational envelop.
c) If b) is not feasible, design multiple optimal PID controllers at specified operating points.
d) Use fuzzy gain scheduling to develop a controller for the output within the specified operational range of the nonlinear plant.

The main time domain specifications were taken as the rise time (t_r) <10 s, settling time (t_s) < 20s, and peak overshoot (PO) < 1%. The maximum surge velocity of the ROV was 1.1 m/s, but due to instability in the vertical plane with surge velocity, the practical maximum value used was 0.75 m/s.

B. *Constraint Optimization*

The individual PID controller was tuned using constraint optimization. The constraints are formulated as a feasibility problem, thus the optimization algorithm finds parameter values that satisfy all constraints to within specified tolerances but does not minimize any objective or cost function in doing so [14]. The feasible region is defined by six inequality and two equality constraints as shown in Fig. 2.

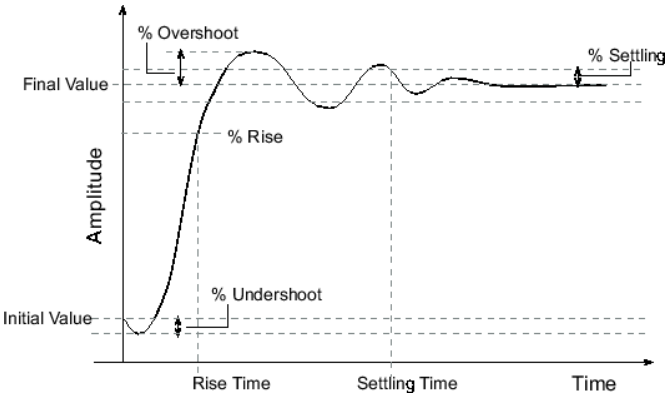

Fig. 2: Signal constraints for a unit step input.

These constraints are piecewise linear bounds (defined as y_{bnd}, with *n* edges) and is represented as,

$$y_{bnd}(t) = \begin{cases} y_1(t) & t_1 \le t \le t_2 \\ y_2(t) & t_2 \le t \le t_3 \\ \vdots & \vdots \\ y_n(t) & t_n \le t \le t_{n+1} \end{cases}, \quad (10)$$

The software computes the signed distance between the simulated response and the edge. The signed distance for the lower bounds is,

$$c = \begin{bmatrix} \max\limits_{t_1 \le t \le t_2} y_{bnd} - y_{sim} \\ \max\limits_{t_2 \le t \le t_3} y_{bnd} - y_{sim} \\ \max\limits_{t_n \le t \le t_{n+1}} y_{bnd} - y_{sim} \end{bmatrix}, \quad (11)$$

where y_{sim} is the simulated response and is a function of the parameters being optimized. The signed distance for the upper bounds is,

$$c = \begin{bmatrix} \max\limits_{t_1 \le t \le t_2} y_{sim} - y_{bnd} \\ \max\limits_{t_2 \le t \le t_3} y_{sim} - y_{bnd} \\ \max\limits_{t_n \le t \le t_{n+1}} y_{sim} - y_{bnd} \end{bmatrix}. \quad (12)$$

If all the constraints are met for some combination of parameter values, then that solution is said to be feasible.

C. Methodology

A MATLAB/Simulink environment was used to develop a 6-DOF dynamic model of the ROV. The Simulink Design Optimization (SDO) toolbox in conjunction with MATLAB Optimization and Global Optimization toolboxes was used to optimize the step response of the system. The SDO provided a Check Step Response Characteristics Block to implement constraints on the output signal. This block, by default provides options to select the gradient-based optimization method (*fmincon*) to optimize the response. However, if the Global Optimization toolbox is installed, then Pattern Search and Simplex methods are also available as choices. The constraints implemented in the Simulink Check Step Response Characteristics Block are shown in Fig. 3. The white area in this figure shows the feasible region for this problem.

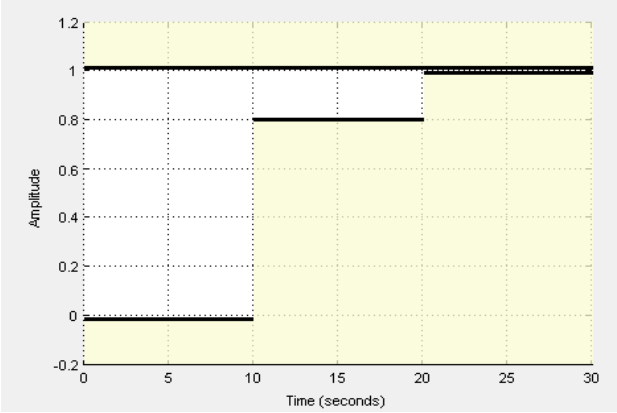

Fig. 3: Constraints in check step response block.

D. Heading Controller

As the first step the model was linearized at a specific operating point defined by the surge velocity of 0.4 m/s. A rough set of gains were obtained for the PID controller using this model, which were then used as the initial guesses for the optimization process. The design gains were selected as proportional ($K_{p)}$, derivative ($K_{d)}$ and integral ($K_{i)}$. Appropriate bounds on design variables were used to limit the search time of the optimizer. These bounds were selected based on control engineers experience and adjusted based on various optimization runs. While the heading measurement would have been sufficient for designing a PID controller, it is well known that large values of K_d could amplify measurement noise. On the other hand, the derivative action can be used to provide additional phase margin and thus increased robustness. In this case, the actual vehicle has a compass to measure the heading and a rate sensor to measure the yaw rate. Therefore, the control law was simply taken to be,

$$u = K_p(\psi_d - \psi) + K_i \int (\psi_d - \psi)dt - K_d r \qquad (13)$$

The optimally tuned gains were $K_p = 15, K_i = 0.01, and\ K_d = 50$. These values gave step responses within the specified characteristics, even at different operating points denoted by different surge speeds. Therefore, further improvement was not required and it was adopted as the heading controller. The simulated results for a heading change of 60 degrees at 3 different speeds are shown in Fig. 4, while a comparison against the Zeigler-Nicholas (ZN) tuning method is shown in Fig. 5, which clearly shows that for ZN tuning PO ≈ 50% and t_s>200s. These are well outside our requirement compared to optimization tuning which shows the superiority of the proposed method over the conventional tuning methods.

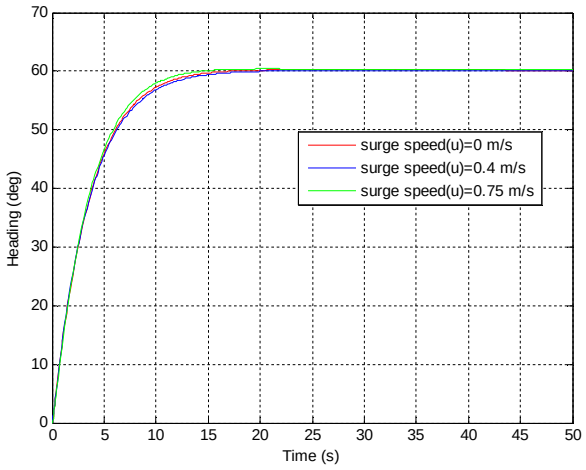

Fig. 4: 60 deg heading at different surge speeds.

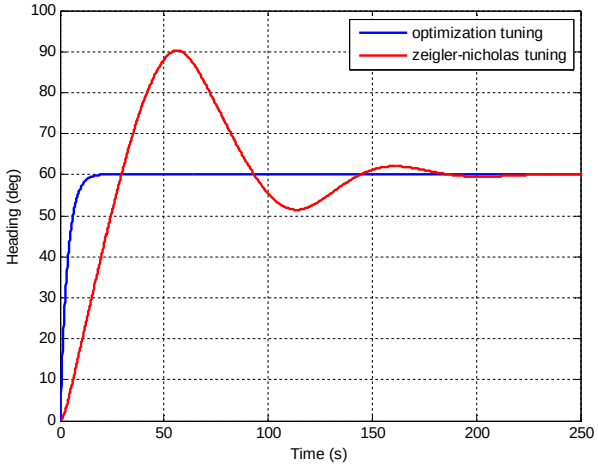

Fig. 5: Comparison of optimized and ZN tuning.

E. Depth Controller

As the vehicle has only a depth sensor, derivative action must be preceded by a low-pass filter $h(t)$ to overcome the amplification of noise. Thus, the control law is taken as,

$$u = K_p(d_d - d) + K_i \int (d_d - d)\,dt + K_d \frac{d}{dt}(d_d - d) * h(t) \quad (14)$$

$$H(s) = \frac{1}{0.005s + 1} \quad (15)$$

Following the same procedure as the heading controller explained earlier, the optimally tuned gains for the depth controller at an operating point of 0.4 m/s were obtained as K_p=15.60, K_i=0.003, and K_d=20. These were used in the numerical simulation model, with Fig. 7 showing the depth change of 1 m at the selected operating point. However, simulation results at other operating points given in Fig. 8 for a depth change of 1 m show that the response does not satisfy the design requirements. It is also seen that the nonlinearity is much more severe at higher velocities than at the lower values. Thus, optimal tuning was carried out at those two operating points as well as at u=0.6 m/s to include more points in the higher velocity range. The values of control gains obtained from the optimization for each operating point satisfying the design criteria are given in Table 1.

TABLE I. PID TUNING TABLE

	u=0 m/s	u=0.4 m/s	u=0.6 m/s	u=0.75m/s
K_p	3.54	15.60	27.88	59.50
K_d	17	20	20	20
K_i	0.003	0.003	0.2	1.85

Finally the fuzzy gain scheduling supervisor was designed using the MATLAB fuzzy control toolbox. For the supervisor design, the following steps were carried out:

1) The membership functions for the input variable were designed using triangular function to maintain simplicity. The operating regions are defined in the universe of discourse of the input by means of overlapping membership functions with vertex of unitary membership grade centred on each set-point value and base positioned on the adjacent set-point values.
2) The PID control gains which are the supervisor outputs were defined by singletons according to Sugeno fussy model.
3) The rules were set based on the tuning table.
4) The selected inference technique is the classical max-min method and the defuzzification scheme is the weighted average.

The membership functions of the input speed were defined as four different membership functions as shown in Fig. 6 covering the entire speed range of 0 to 0.75 m/s as,

a) Slow [-0.4 0 0.4]
b) Medium [0 0.4 0.6]
c) Medium fast [0.4 0.6 0.75]
d) Fast [0.6 0.75 0.9].

In order to allocate the correct controller gains, a set of rules were created as follows.

If (speed ∈ A) then (K_p is a) and (K_d is b), and (K_i is c), where A is a fuzzy set and a, b, and c are constants.

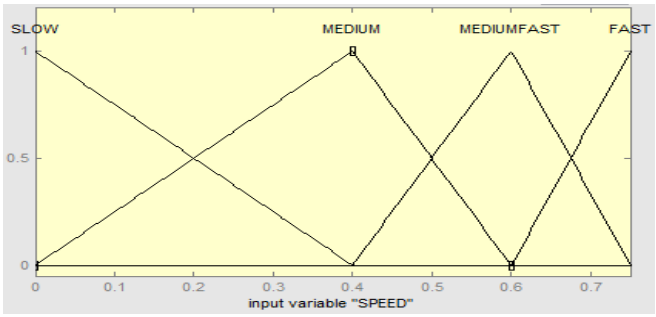

Fig. 6: Input surge velocity membership functions.

Simulation results for depth change of 1 m at three speeds for which the gains were inferred using fuzzy rules are shown in Fig. 9. They show that the response at different surge velocities of the fuzzy controller is satisfactory, with only the peak overshoot increasing slightly but still less than 2%.

IV. MEASUREMENT NOISE

In both controllers the feedback is provided by measurement using on-board sensors. A measured signal can be represented as:

$$x_{measured} = x_{original} + e_s + e_r \quad (16)$$

where $x_{original}$ is the true value of the variable that is being measured, e_s is the systematic error, and e_r is the random error. The systematic error is a variable offset from the x value due to inherent inaccuracies within the sensor such as poor sensor calibration. Random error, sometimes referred to as measurement noise, can be due to many factors, but for sensors it is often caused by electromagnetic interference. A feature of this random error is for the mean to tend to zero as time tends towards infinity.

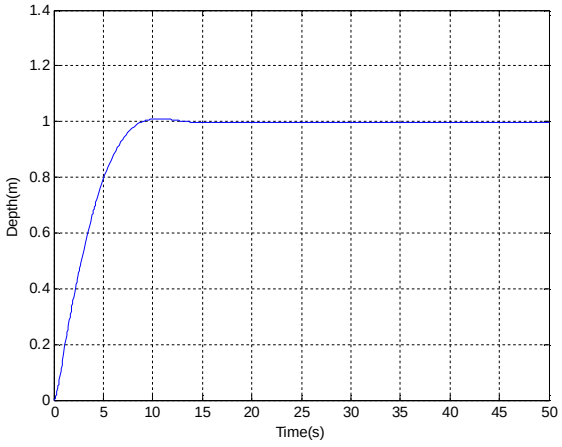

Fig. 7: 1m depth change at u=0.4m/s by optimal PID controller.

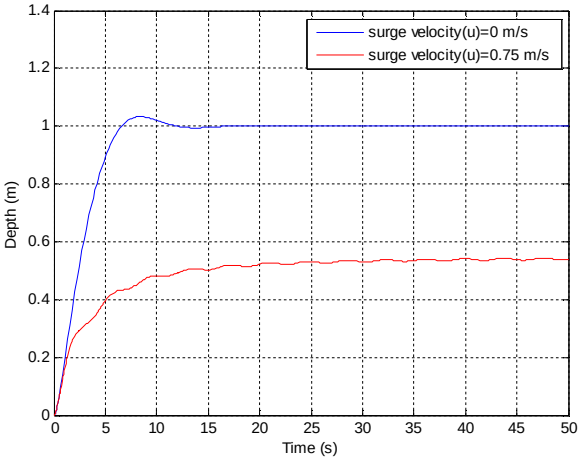

Fig. 8: 1m depth change at two different points.

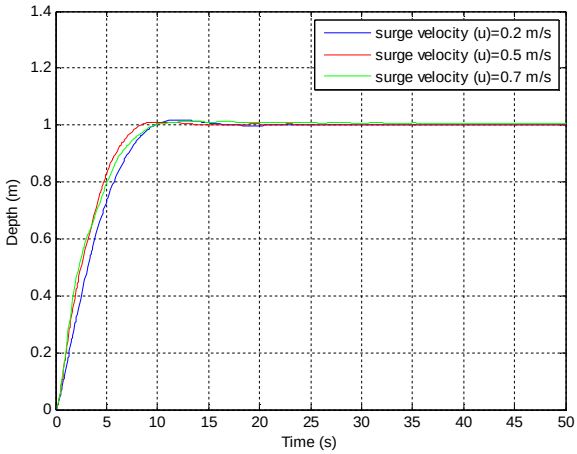

.

Fig. 9: 1m depth change by fuzzy controller .

In order to verify the robustness of the controller, the effect of random noise on the performance of the optimally tuned PID controllers was investigated. Thus, the random noise with a Gaussian distribution was added to the depth, heading, and yaw rate signals from the non-linear model. The magnitude of this additional measurement noise was quantified by its standard deviation, which was set to 0.001 for both the depth and heading signals. The response of the simulation to depth change with the inclusion of noise is shown in Fig. 10.

Fig. 10 shows that apart from the fluctuation due to noise, there are no significant disturbances causing erratic, unacceptable performance. Comparing this result with those obtained for the model predictive control with similar noise levels by Steenson, et al. [15], it is clear that the controllers developed in this work are sufficiently robust to measurement noise.

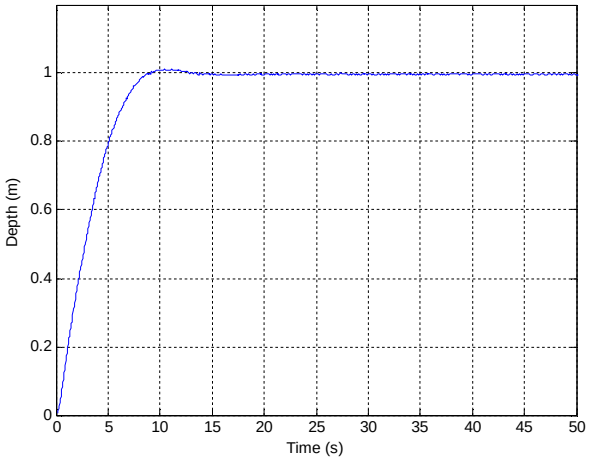

Fig 10. 1 m depth change with measurment noise

V. CONCLUSION

The paper has presented the heading and depth controller for a UUV by optimization of PID gains based on the nonlinear dynamics of the vehicle. The simulation results show that the PID controller has excellent performance with respect to the heading control, while fuzzy gain scheduling was required for the depth controller due to severe nonlinearities in the vertical plane. Moreover, when low levels of measurement noise were added to the feedback signals, the performance remained within acceptable levels. Future work will focus on optimizing the membership functions.

REFERENCES

[1] D. A. Smallwood and L. L. Whitcomb, "Model-based dynamic positioning of underwater robotic vehicles: theory and experiment," in IEEE Journal of Oceanic Engineering, 2004, pp. 169-186.

[2] L. Hsu, "Dynamic positioning of remotely operated underwater vehicles," IEEE Robotics and Automation Magazine, vol. 7, pp. 21-31, 2000.

[3] J. N. Lygouras, "DC thruster controller implementation with integral anti-wind up compensator for underwater ROV," Journal of Intelligent and Robotic Systems: Theory and Applications, vol. 25, pp. 79-94, 1999.

[4] T. H. Koh, M. W. S. Lau, G. Seet, and E. Low, "A control module scheme for an underactuated underwater robotic vehicle," Journal of Intelligent and Robotic Systems: Theory and Applications, vol. 46, pp. 43-58, 2006.

[5] D. R. Yoerger, J. J. E. Slotine, J. Newman, and H. Schempf, "Robust trajectory control of underwater vehicles," in Unmanned Untethered Submersible Technology, Proceedings of the 1985 4th International Symposiumon,1985,pp.184-197.

[6] D. R. Yoerger and J.-J. E. Slotine, "Adaptive sliding control of an experimental underwater vehicle," in Proceedings of the 1991 IEEE International Conference on Robotics and Automation, April 9, 1991 - April 11, 1991, Sacramento, CA, USA, 1991, pp. 2746-2751.

[7] A. J. Healey and D. Lienard, "Multivariable sliding mode control for autonomous diving and steering of unmanned underwater vehicles," IEEE Journal of Oceanic Engineering, vol. 18, pp. 327-339, 1993.

[8] D. Fryxell, P. Oliveira, A. Pascoal, C. Silvestre, and I. Kaminer, "Navigation, guidance and control of AUVs: an application to the

Marius vehicle," Control Engineering Practice, vol. 4, pp. 401-409, 1996.

[9] A. Pascoal, P. Oliveira, C. Silvestre, A. Bjerrum, A. Ishoy, J.-P. Pignon, G. Ayela, and C. Petzelt, "MARIUS: An autonomous underwater vehicle for coastal oceanography," IEEE Robotics and Automation Magazine, vol. 4, pp. 46-59, 1997.

[10] A. Pascoal, C. Silvestre, and P. Oliveira, "Vehicle and mission control of single and multiple autonomous marine robots," Advances in Unmanned Marine Vehicles,IEE Control Engineering Series, vol. 69, pp. 353-386, 2006.

[11] W.-J. Chang, W. Chang, and H.-H. Liu, "Model-based fuzzy modeling and control for autonomous underwater vehicles in the horizontal plane," Journal of Marine Science and Technology, vol. 11, pp. 155-163, 2003.

[12] S. W. Jun, D. W. Kim, and H. J. Lee, "Design of T-S fuzzy-model-based controller for depth control of autonomous underwater vehicles with parametric uncertainties," in 2011 11th International Conference on Control, Automation and Systems, ICCAS 2011, October 26, 2011 - October 29, 2011, Gyeonggi-do, Korea, Republic of, 2011, pp. 1682-1684.

[13] T. I. Fossen, Guidance and Control of Ocean Vehicles: John Wiley and Sons Ltd, 1994.

[14] Matlab, Optimization Toolbox Users Manual.

[15] Steenson, L.V.; Phillips, A.B.; Turnock, S.R.; Furlong, M.E.; Rogers, E., "Effect of measurement noise on the performance of a depth and pitch controller using the model predictive control method," Autonomous Underwater Vehicles (AUV), 2012 IEEE/OES , vol., no., pp.1,8, 24-27 Sept. 2012